Desalination and Water Treatment
www.deswater.com

doi: 10.5004/dwt.2018.23075

136 (2018) 157–166
December

Investigation of a new double-hydrophilic block terpolymer as calcium scale inhibitors and dispersants

Yiyi Chen[a], Qiuli Nan[b], Yongjuan Wang[a], Yuming Zhou[a,b,*], Qingzhao Yao[a,*], Mingjue Zhang[b], Wei Sun[c]

[a]*School of Chemistry and Chemical Engineering, Southeast University, Nanjing 211189, China, Tel. +86 25 52090617; emails: ymzhou@seu.edu.cn (Y. Zhou), 101006377@seu.edu.cn (Q. Yao), chenyiyi0220@126.com (Y. Chen), 562655117@qq.com (Y. Wang)*
[b]*School of Chemical and Pharmaceutical Engineering, Southeast University Chengxian College, Nanjing 210032, China, Tel. +86 25 52090617; emails: 53212651@qq.com (Q. Nan), 489354839@qq.com (M. Zhang)*
[c]*Jianghai Environmental Protection Co., Ltd., Changzhou 213116, China; email: leojhhg@sina.com*

Received 13 March 2018; Accepted 5 September 2018

ABSTRACT

In the circulating cooling water systems, scale formation and stabilization of suspensions are persistent problems, which can be overcome through the use of water-soluble polymers. In this work, a new double-hydrophilic block terpolymer AA-APES-H_3PO_3 was synthesized from the monomers of acrylic acid (AA), ammonium allylpolyethoxy sulfate (APES), and phosphorous acid (H_3PO_3) with water as solvent by the free-radical polymerization. This terpolymer AA-APES-H_3PO_3 was characterized by Fourier-transform infrared spectrometry (FT-IR) and nuclear magnetic resonance spectroscopy. The performances of AA-APES-H_3PO_3 on the inhibition of $CaCO_3$ and $CaSO_4$ and its dispersion ability on Fe_2O_3 were also studied. The results show that the inhibition efficiency of AA-APES-H_3PO_3 is close to 93% for $CaCO_3$ with 8 mg/L inhibitor, and reach up to 100% for $CaSO_4$ with 4 mg/L inhibitor. The best dispersion efficiency for ferric oxide is 19.4% when AA-APES-H_3PO_3 is 16 mg/L. Scanning electronic microscopy, X-ray powder diffraction analysis and FT-IR were used to investigate the effect on morphology of $CaCO_3$ and $CaSO_4$ scales, which were highly modified in the presence of AA-APES-H_3PO_3. The proposed inhibition mechanism suggests that sulfo groups improved inhibitory activity and dispersion ability and showed higher calcium ion tolerance, while terpolymer containing poly(ethylene glycol) segments, –COOH, increased its solubility in water.

Keywords: Terpolymer; Scale inhibition; Calcium carbonate; Calcium sulfate; Dispersity

1. Introduction

In recent years, the formation of sparingly soluble salts in industrial circulating cooling water systems is a serious problem, often weakening the heat exchange, shortening the life of equipment and in all cases increasing the cost of production [1]. The commonly occurring scales, such as calcium carbonate, calcium sulfate, and calcium phosphate, have a strong appeal to the researchers and they have worked on various solutions to inhibit scale formation and precipitation for many years [2,3]. Among those strategies, chemical and physical methods are mainly used. While the addition of scale inhibitors is one of the most common applied chemical methods to prevent or control scale deposition [4,5].

Over the past years, more attention was paid to copolymer scale inhibitors because of their multi-functional groups (such as carboxylate, phosphonate, sulfonate,

* Corresponding authors.

etc.) and excellent inhibition and dispersity properties [6,7]. Poly(acrylic acid) (PAA), hydrolyzed poly(maleic anhydride) (HPMA), and poly(epoxysuccinic acid) (PESA) are usually used as carbonate scale inhibitors with good chelating ability and dispersability [8]. Also they can be safely used up to a high temperature and a high value of pH at a very low dosage level [5]. However, as they only contain carboxylic groups and lack more hydrophilic groups, the existing shortages are the poor comprehensive scale inhibition performance, a low calcium tolerance, and the formation of calcium micelles, which limit their use and decrease the efficiency [1,9]. Phosphorous scale inhibitors, such as 1, 2-diaminoethanetetrakis-methylene phosphonic acid (EDTMP) and 1-hydroxy ethylidine-1,1-diphosphonic acid (HEDP), have also been used satisfactorily because they can adsorb onto the metal surface strongly and prevent precipitation [10.]. Nevertheless, these phosphonate inhibitors are easy to hydrolyze and convert to orthophosphate, which will react with calcium ions to form indissolvable calcium phosphate scale. Furthermore, phosphorous will serve as nutrients for algae when discharging with wastewater [7,9]. Therefore, considering the environmental pollution and ecological imbalance in water, it is extremely urgent to develop ecologically benign scale and corrosion inhibitors, which will gradually replace the application of high levels of phosphonates in water treatment systems [11,12].

In the circulating cooling water systems, cooling water will be contaminated with various forms of oxidized iron due to the corrosion of steel equipment and/or its introduction with feedwater. Generally, Fe(II) ions have very high solubility in an aqueous medium and pose no challenges for the system at low pH values from 3 to 4. However, when the pH value increases to 5 or above, Fe(II) ions, being oxidized to Fe(III) ions, will go through hydrolysis to form iron hydroxide ($Fe(OH)_3$) or iron oxide (Fe_2O_3), which will deposit onto the surface of the pipe and reduce the heat transfer efficiency and cause corrosion scales [13]. So maintaining the oxidized iron in soluble or in dispersed forms can probably prevent heat exchanger surfaces fouling [14].

Due to its high electron density of oxygen atoms and high polarity, the sulfonic groups have strong adsorption capacity and high electrostatic repulsion, which means the polymer containing sulfonic groups can play a role in the inhibition and dispersion stability [15,16]. Therefore, the sulfonic groups have been introduced into the polymer.

In this work, we synthesized a new environmental friendly multi-functional scale inhibitor AA-APES-H_3PO_3 terpolymer, containing carboxylic groups, poly(ethylene glycol) (PEG) segments, sulfonic groups, amide groups and phosphonyl. This terpolymer was prepared from the monomers of acrylic acid (AA), ammonium allylpolyethoxy sulfate (APES), and phosphorous acid (H_3PO_3) with water as solvent and redox system of hypophosphorous and ammonium persulfate as initiator by the free-radical polymerization. The method of energy-dispersive X-ray analysis was used to measure the content of phosphorous in the synthesized terpolymer. Results showed that the mass percentage of phosphorous was less than 1.5%, indicating AA-APES-H_3PO_3 is the low-phosphorous terpolymer. The chemical structure of the terpolymer was characterized by Fourier-transform infrared spectrometry (FT-IR) and ^{1}H-NMR. The most important goal of this study is to determine the scale inhibition effect of AA-APES-H_3PO_3 terpolymer against $CaCO_3$ and $CaSO_4$ scales through the method of static scale inhibition test and dispersing ability in the artificial cooling water. The influence of AA-APES-H_3PO_3 terpolymer on the morphology of $CaCO_3$ and $CaSO_4$ precipitations was investigated through scanning electron microscopy (SEM), X-ray diffractometer (XRD), and FT-IR, respectively.

2. Experimental procedure

2.1. Reagents

APES was synthesized from allyloxy polyethoxy ether in our laboratory according to Du et al. [17,18]. The chemical reagents used were analytical grade AA, phosphorous acid (H_3PO_3), ammonium persulfate, calcium chloride, sodium bicarbonate, sodium sulfate, sodium borate, and ferrous sulfate, which were all obtained from Zhongdong Chemical Reagent Co., Ltd. (Nanjing, China). AA-APEM-H_3PO_3 was synthesized from APEM in our laboratory according to our previous studies [13]. Commercial inhibitors of HPMA (600 MW), HEDP (206 MW), PESA (1,500 MW), and EDTMP (436 MW) were in technical grade and supplied by Jiangsu Jianghai Chemical Co., Ltd. (Changzhou, China). Deionized (DI) water was used throughout the experiments.

2.2. Synthesis of AA-APES-H_3PO_3 terpolymer

A 4-neck round bottom flask, equipped with a thermometer, a mechanical stirrer, and a reflux condenser, was charged with 40 mL of DI water and 0.5 mol of AA and heated to the reaction temperature 80°C over a period of time under nitrogen atmosphere. After that, a mixture of the raw materials APES and H_3PO_3 was added in 25 mL of DI water. In mixed conditions, the initiator ammonium persulfate was dropped at a constant flow rate separately for about 1 h. The reaction was then heated to 90°C and maintained at this temperature for an additional 1.5 h, eventually obtaining an aqueous polymer solution containing approximately 20.3% solid. The synthesis procedure of the terpolymer is given in Fig. 1.

2.3. Characterization of AA-APES-H_3PO_3 terpolymer

The structures of APES and AA-APES-H_3PO_3 were analyzed by FT-IR spectroscopy (VECTOR-22, Bruker Co., Germany) in the region of 4,000–500 cm^{-1}. About 1 mg of dried samples was mixed with 100 mg of dried KBr powder and then compressed into a disk for spectrum recording. A Bruker nuclear magnetic resonance (NMR) analyzer (AVANCE AV-500, Bruker, Switzerland) was also used to explore the structures of samples, operating at 500 MHz. Thermogravimetric analysis (TGA) was performed on APES and AA-APES-H_3PO_3 at temperatures ranging from 20°C to 700°C. Such signals were obtained at a heating rate of 20°C/min in a nitrogen atmosphere using a PerkinElmer Derivatograph instrument (PerkinElmer, USA).

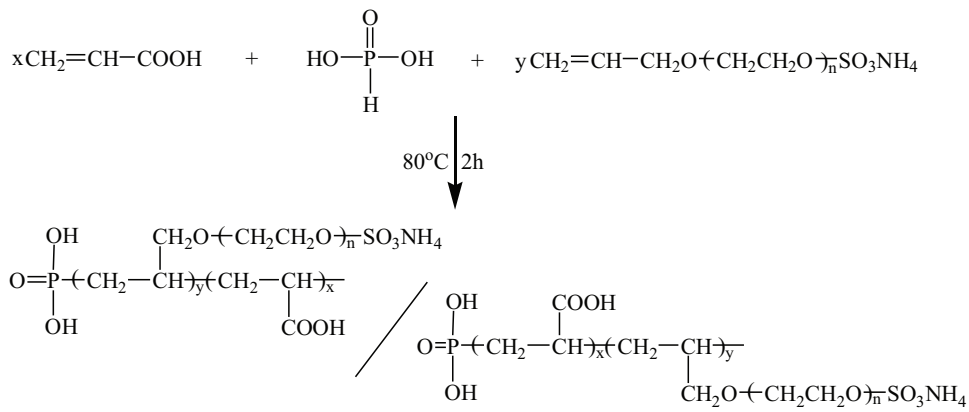

Fig. 1. Synthesis procedure of AA-APES-H_3PO_3.

2.4. Evaluation of AA-APES-H_3PO_3 terpolymer

2.4.1. The efficiency of static scale inhibition against $CaCO_3$ scale and $CaSO_4$ scale

The inhibition performance of AA-APES-H_3PO_3 terpolymer for $CaCO_3$ and $CaSO_4$ scales is determined according to the China National Standard (GB/T16632-2008) by the static test method. The experimental conditions of $CaCO_3$ were $\rho(Ca^{2+})$ = 240 mg/L, $\rho(HCO_3^-)$ = 736 mg/L (as $CaCO_3$), and the solutions were maintained at 80°C for 10 h in water bath. The remaining Ca^{2+} in the supernatant was titrated by ethylene diamine tetraacetic acid standard solution and compared with blank test. The inhibition efficiency η was defined as follows:

$$\eta = \frac{\rho_1(Ca^{2+}) - \rho_2(Ca^{2+})}{\rho_0(Ca^{2+}) - \rho_2(Ca^{2+})} \times 100\% \quad (1)$$

where ρ_0 (Ca^{2+}) is the total concentrations of Ca^{2+} (mg/L), ρ_1 (Ca^{2+}) is the concentrations of Ca^{2+} (mg/L) in the presence of the terpolymer inhibitor, and ρ_2 (Ca^{2+}) is the concentrations of Ca^{2+} (mg/L) in the absence of the terpolymer inhibitor.

Procedure of $CaSO_4$ precipitation experiments was also carried out similarly to $CaCO_3$ precipitation experiments, according to the national standard of China concerning the code for the design of industrial oil field–water treatments (SY/T 5673-93). $CaSO_4$ was formed from supersaturated solutions prepared by mixing of 250 mL $CaCl_2$ and Na_2SO_4 solutions. Then the specimen was heated in a water bath at 60°C for 6 h and the determination of Ca^{2+} was carried out by exactly same process.

2.4.2. The performance of dispersing ferric oxide

The iron-dispersing ability was tested through UV–visible studies. Confecting water for the experiment was prepared by adding a known volume of calcium stock solution and iron (II) stock solution to a beaker (1,000 mL) with a certain amount of water, at room temperature under continuous stirring. The final concentration of Ca^{2+} was 150 mg/L, while Fe(II) ion concentration was 10 mg/L. The pH value of the solution was adjusted to 9.0 by using borax and then the solution was mixed with a known amount of the terpolymer AA-APES-H_3PO_3. Mixed solution was stirred for 15 min and maintained at 50°C for 5 h. The transmittance of the supernatant was measured with 722-spectrophotometer under the wavelength of 420 nm. The lower the light transmittance is, the better is the terpolymer efficacy, as an iron (III) inhibitor.

2.4.3. Crystal characterization

The solids precipitated were characterized by SEM (S-3400N, HITECH) and powder XRD (Siemens D5000 diffractometer). The samples examined by SEM were coated with a layer of gold. Precipitated phases were identified by XRD on a Rigaku D/max 2400 XRD with Cu Ka (k51.5406) radiation (40 kV, 120 mA). The FT-IR spectra of $CaCO_3$ crystal over the wave number range 4,000–500 cm^{-1} were recorded using a FT-IR spectrometer.

3. Results and discussion

3.1. GPC analysis of AA-APES-H_3PO_3

It is well known that the structure of polymer is affected by the M_w, and M_w is an important parameter in the process of scale inhibition. The weight distribution of the polymer was measured by gel permeation chromatography (GPC, calibrated with PEG standards) at the 1.0 mL/min run flow rate. After analysis of the GPC results, we found that the weight-average molecular weight (M_w) was 1.70 × 10^4, whereas the number-average molecular weight (M_n) was 1.63 × 10^4. Thus, we obtained a polydispersity index (PD) of 1.04 (PD = M_w/M_n).

3.2. FT-IR and ^{1}H-NMR analysis of AA-APES-H_3PO_3

To make sure that the terpolymer has been obtained, the FT-IR spectra of (a) APES and (b) AA-APES-H_3PO_3 were measured, the results are shown in Fig. 2. From the spectrum of APES, the absorption peak at 1,648 cm^{-1} is assigned to the stretching vibration of C = C; the peak at 1,352 cm^{-1} is assigned to the asymmetric stretching vibration of S = O; and the peak at 1,100 cm^{-1} is attributed to the asymmetric stretching vibration of C–O–C. While in the spectrum of AA-APES-H_3PO_3 terpolymer, the peak at 1,724 cm^{-1} is

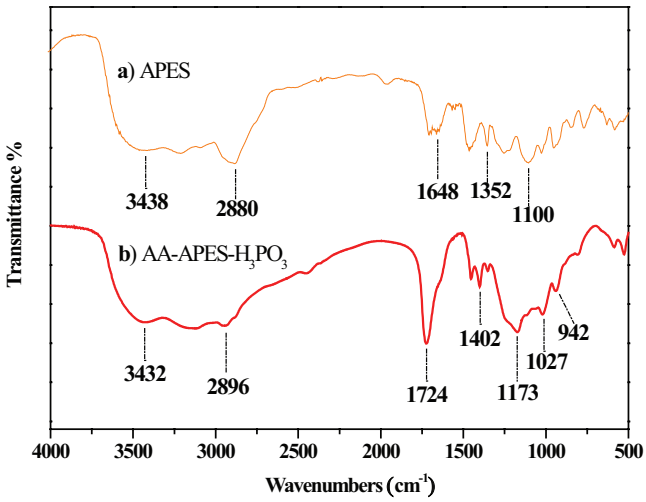

Fig. 2. The FT-IR spectra of (a) APES and (b) AA-APES-H_3PO_3 terpolymer.

assigned to the stretching vibration of C = O; the absorption peak at 1,402 cm^{-1} is attributed to the vibration of C–P [4]; the peak at 1,173 cm^{-1} is assigned to the stretching vibration of P=O; the peak at 1,027 cm^{-1} and 942 cm^{-1} are attributed to the stretching vibration of P–O. Meanwhile, the stretching vibration of N–H appears at 3,438 and 3,432 cm^{-1} in both spectrum, and 2,880 and 2,896 cm^{-1} are characteristic absorption peaks of saturated methane. The existence of C–P absorption peak at 1,402 cm^{-1} and the disappearance of C=C absorption at 1,648 cm^{-1} indicate that free radical polymerization of monomers is completed [19]. Based on all those facts, it can be sure that the terpolymer has carboxylic acid group, sulfonic acid group, amide group and phosphino group.

The structure of raw material and the synthesized terpolymer was characterized by ^{1}H-NMR with deuterated dimethyl sulfoxide as the solvent and the corresponding spectra are exhibited in Fig. 3. According to the data, the peak at 2.50 is assigned to the solvent residual peak of $(CD_3)_2SO$. The chemical shifts in the region of 4–6 ppm are assigned to

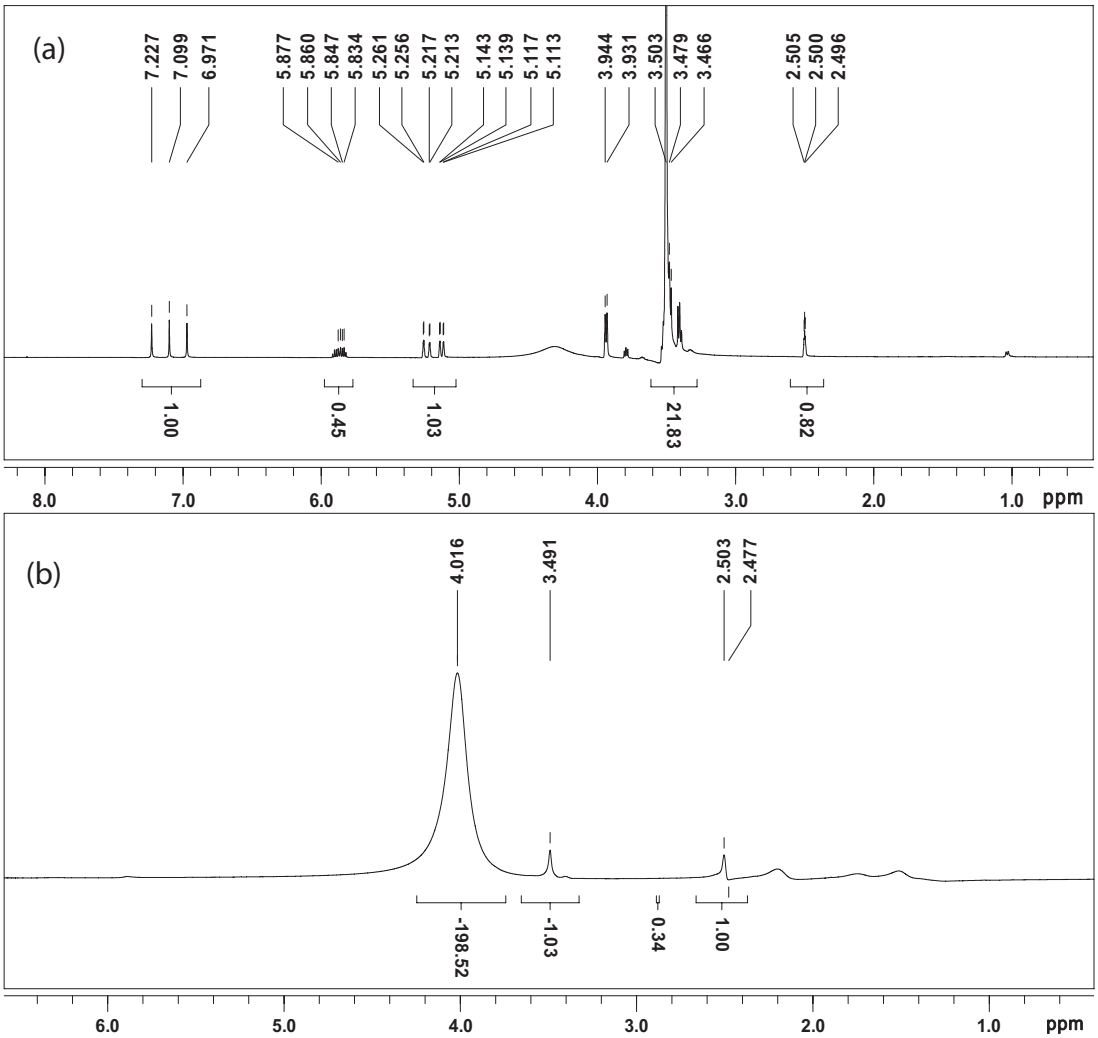

Fig. 3. The ^{1}H-NMR spectra of (a) APES and (b) AA-APES-H_3PO_3 terpolymer.

propenyl protons (CH_2=CH–CH_2–) in Curve (a), and there are no peaks in this range in Curve (b), which is consistent with the results of FT-IR analysis. The double bond absorption peaks completely disappear, revealing that the free radical polymerization between AA and APES has occurred. Therefore, the terpolymer AA-APES-H_3PO_3 was synthesized successfully.

3.3. Characterization by TGA

TGA was used to investigate the thermal stability of the terpolymer and obtain further information on the structures of APES and AA-APES-H_3PO_3. The corresponding curves are depicted in Fig. 4. The data listed show that the degradation of APES and AA-APES-H_3PO_3 all proceeded in two or three stages. The first decomposition stage was assigned to the removal of volatile matter existing in these samples, such as entrapped moisture or extraction solvent. AA-APES-H_3PO_3 undergoes about 80% of weight loss at up to 100°C, according with its solid content. The greatest percentage decomposition of APES occurred in the second stage (180°C–400°C), as indicated by the corresponding weight loss values. At high temperatures, it may be attributed to cracking, gasification or carbonization [20].

3.4. Influence of AA-APES-H_3PO_3 dosage on $CaCO_3$ inhibition

The calcium carbonate scale inhibition performance of AA-APES-H_3PO_3 in simulated scale inhibition solution was tested at different concentrations, as shown in Fig. 5. First of all, as can be seen that the inhibition efficiency is strongly affected by the concentration of terpolymer. The increase of the inhibition efficiency is obvious with AA-APES-H_3PO_3 concentration rising from 2 to 8 mg/L, after that the inhibition efficiency remains nearly unchanged with further increase in the concentration. It is also observed that there is a threshold effect at a level of 8 mg/L. Because the carboxylic ion adsorbs on $CaCO_3$ crystal at 80°C, the adsorption equilibrium (chemisorption) appears, usually strong and irreversible [21].

Furthermore, the ability of several copolymers containing different functional groups was also tested at the identical conditions, including AA-APEM-H_3PO_3, EDTMP, HEDP, PESA and PAA. It can be shown that the order of preventing the precipitation is AA-APES-H_3PO_3 > AA-APEM-H_3PO_3 > EDTMP > HEDP > PESA > PAA. Compared with AA-APEM-H_3PO_3, AA-APES-H_3PO_3 performs much better in inhibiting $CaCO_3$ formation as it contains additional sufonic group and amide group. It is evident that polymer performance strongly depends upon the functional groups present in the polymers. It is also worth mentioning that phosphonates, such as EDTMP and HEDP, effective inhibitors on calcium carbonate deposits, display significant ability to control calcium carbonate scales and their inhibition is superior to that of the other investigated nonphosphorous inhibitors, PESA and PAA, which contain only carboxyl groups and can hardly control calcium carbonate scales even at high dosages, as is apparent from Fig. 5. Therefore, it can be seen that the inhibitor AA-APES-H_3PO_3 displays the best ability to control calcium carbonate scales among those inhibitors investigated. These facts suggest that the side-chain PEG, sulfonic group (SO_3) segments of APES and carboxyl groups of AA might play an important role during the control of $CaCO_3$ scales.

3.5. Influence of AA-APES-H_3PO_3 dosage on $CaSO_4$ inhibition

The inhibition efficiency of AA-APES-H_3PO_3, AA-APEM-H_3PO_3 and some commercial inhibitors against $CaSO_4$ scale is shown in Table 1. As seen from Table 1, both two terpolymers show good inhibition effects on $CaSO_4$ scale. Similarly, the inhibition efficiency increases with the increasing concentration of inhibitors, and the inhibition efficiency increases dramatically with increasing concentration within a concentration range of 3–4 mg/L. The inhibitors, AA-APES-H_3PO_3 and AA-APEM-H_3PO_3, have threshold dosage of 4 mg/L, and the maximum inhibitory powers are different: 99.5% and 98%. Moreover, the terpolymer AA-APES-H_3PO_3 is extremely effective for preventing the precipitation of $CaSO_4$ deposits, compared with commercial inhibitors.

3.6. Performance of dispersing ferric oxide

The results showing the performance of AA-APES-H_3PO_3 as an iron oxide dispersant at varying dosages are presented in Fig. 6, compared with commercial polymers, PESA and HEDP. Fig. 6 shows that the terpolymer performance

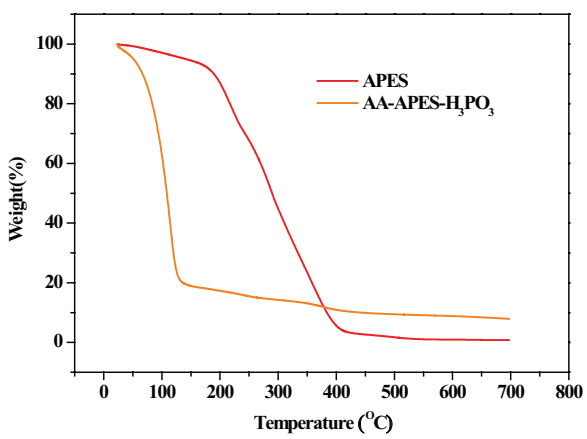

Fig. 4. TGA curves for APES and AA-APES-H_3PO_3 terpolymer.

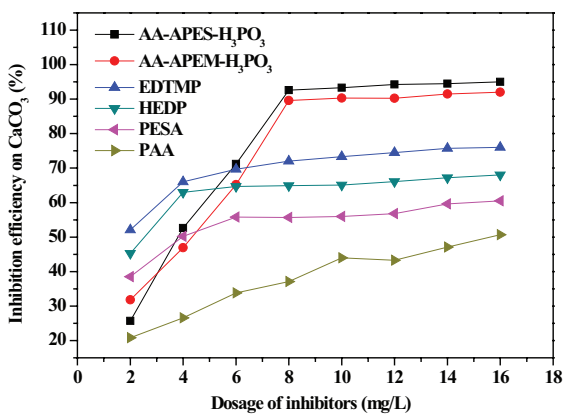

Fig. 5. Scale inhibition of AA-APES-H_3PO_3 and different commercial inhibitors on $CaCO_3$ at different concentrations.

Table 1
Comparison of $CaSO_4$ inhibition

Inhibition on $CaSO_4$ (%)									
Inhibitor type	Dosage (mg/L)								
	1	2	3	4	5	6	7	8	9
AA-APES-H_3PO_3	28.6	60.2	80.5	97.9	98.2	99	99.2	99.3	99.5
AA-APEM-H_3PO_3	23.4	48.8	70.3	95.3	96.5	97	97.1	98.3	98
EDTMP	15	21.7	39.2	33.1	38.7	40.5	56.5	55	58.8
HEDP	30.4	48	53.9	50	57.8	77.1	88.5	84.9	86.3
PESA	19.2	37.4	72.3	70.5	75.9	79.3	78.7	81.1	79.5
PAA	19.8	39	60.4	80.5	80.9	81.3	81.5	81.6	81.8

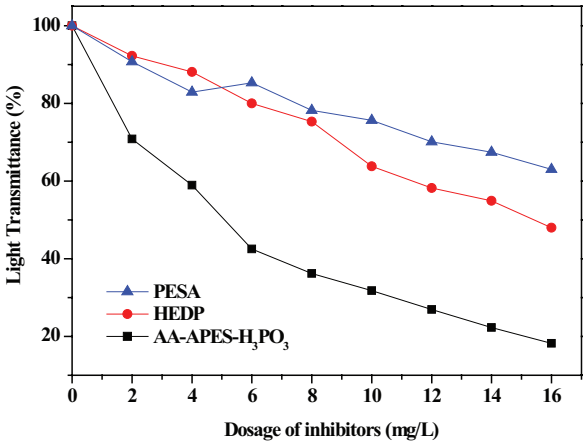

Fig. 6. Ferric oxide dispersion of AA-APES-H_3PO_3, HEDP, and PESA.

strongly depends on polymer dosages. The best dispersion efficiency for ferric oxide is 19.4% when AA-APES-H_3PO_3 is 16 mg/L, while HEDP is 48% and PESA is 63% at the same dosage. So it is obvious that the iron dispersancy of the terpolymer is much better than that of HEDP and PESA. This fact demonstrates that introducing the PEG groups into the structure of terpolymer could improve its dispersion properties on Fe_2O_3. Meanwhile, the photographs, showing the changes of solutions with addition of AA-APES-H_3PO_3, are also depicted in Fig. 7.

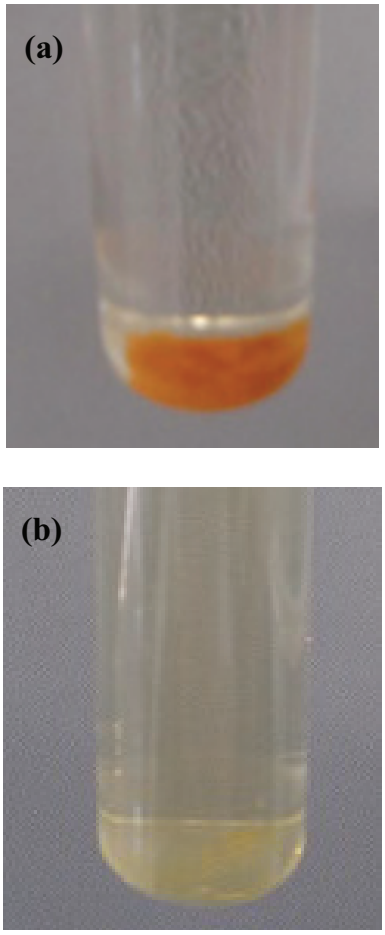

Fig. 7. Photographs of iron solutions in the presence of AA-APES-H_3PO_3 at levels of (a) 0 mg/L and (b) 10 mg/L.

3.7. Characterization of $CaCO_3$ scale

The morphology of collected $CaCO_3$ crystals obtained in the absence and presence of 2, 5 and 8 mg/L of terpolymer were characterized by SEM analysis, as shown in Fig. 8. A special feature of calcium carbonate crystal is polymorphism. It occurs in different crystalline forms in the order of decreasing stability: calcite, aragonite and vaterite [22]. As shown in Fig. 8(a), $CaCO_3$ deposits present calcite structure, which is symmetry and like hexahedron particle with uniform size and glossy surface. Compared with the $CaCO_3$ scales of blank water, scale particles in the presence of AA-APES-H_3PO_3 have changed and oblate spherical shape particles are visible in the SEM image (Fig. 8(b)). When the AA-APES-H_3PO_3 concentration increases to 8 mg/L (Fig. 8(d)), schistose structure takes place of the oblate spherical shape particles, which can make hard scales transforming into soft dirt that can be easily washed away by water at certain water scouring velocity or temperature [9]. The terpolymer AA-APES-H_3PO_3 could dramatically change the morphology of $CaCO_3$ crystals, probably due to the strong specific interaction between crystals and functional groups, which are $–P(O)(OH)_2$, –COOH, $–SO_3$ and PEG groups.

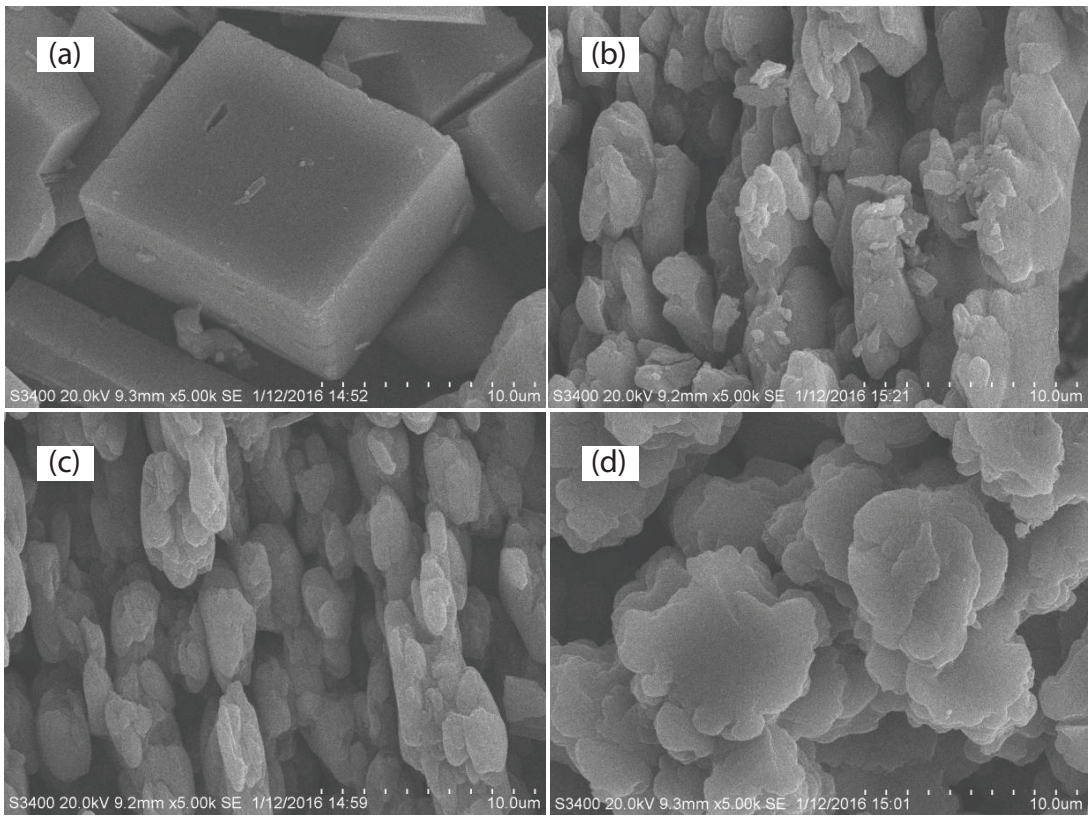

Fig. 8. SEM photographs for (a) $CaCO_3$, (b) with the presence of 2 mg/L, (c) 5 mg/L, and (d) 8 mg/L of AA-APES-H_3PO_3.

The XRD pattern of $CaCO_3$ crystals obtained in the absence and presence of terpolymer is given in Fig. 9. We can see that diffraction peaks of 23.05°, 29.46°, 31.44°, 36.00°, 39.46°, 43.18°, 47.50° and 48.53° in Spectrum (a), which are characteristic peaks of calcite. This result demonstrates that the calcium carbonate scale of blank water is the mixture of calcite, which is the main crystal form, in the absence of AA-APES-H_3PO_3 [23]. In Spectrum (b), there are diffraction peaks of 21.05°, 24.88°, 27.10°, 32.78°, 43.85° and 50.06°, corresponding to vaterite, which is the main crystal form in the presence of AA-APES-H_3PO_3 [24]. These results indicate that the synthesized AA-APES-H_3PO_3 contributes to distortion of $CaCO_3$ crystals and induction of vaterite growth, which is harder to adhere to metal surface and easy to disperse in water solution [25].

FT-IR was also used to confirm the changes of $CaCO_3$ crystal forms, as shown in Fig. 10. The peak at 710 cm^{-1} is attributed to the vibrations of calcite in Curve (a), while the peak at 744 cm^{-1} reflects the feature of vaterite in Curve (b) [26]. These changes are in accord with the results in Figs. 8 and 9.

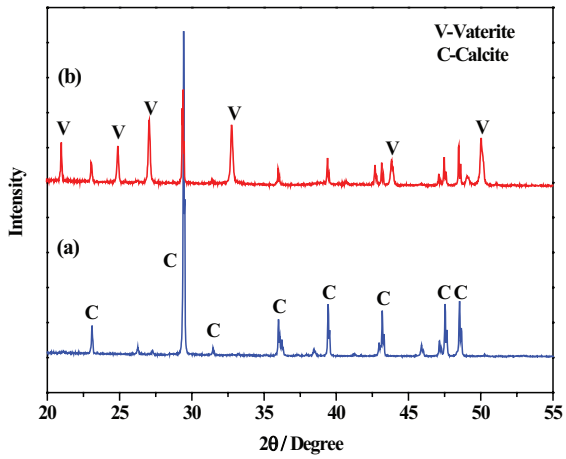

Fig. 9. XRD images for (a) $CaCO_3$ and (b) with the presence of 5 mg/L of AA-APES-H_3PO_3.

3.8. Characterization of $CaSO_4$ scale

The SEM photographs for $CaSO_4$ scales with and without the presence of AA-APES-H_3PO_3 terpolymer are presented in Fig. 11. Among the three types of calcium sulfate crystals, calcium sulfate dihydrate crystal dominates at lower temperature. As shown in Fig. 11(a), calcium sulfate dihydrate crystals are thin tubular cells and needles exhibiting monoclinic symmetry [5,27]. When AA-APES-H_3PO_3 was added to the solution, the shapes of $CaSO_4$ deposits become irregular (Fig. 11(b)). With the increasing of its concentration, the morphology is modified from a needle-shaped structure to smaller, spongy fragments, as seen from Fig. 11(d). The terpolymer causes changes in the original conformation of $CaSO_4$ crystal thus reducing crystallinity and leading to crystal distortion. Such changes cause the calcium sulfate to become loose and prevent formation of fouling, which in turn prevents the deposition on the pipe surface.

Fig. 12 is the XRD spectra for $CaSO_4$ crystals in the (a) absence and in the (b) presence of AA-APES-H_3PO_3. In Spectrum (a), there are strong diffraction peaks at 11.66°, 20.71°, 23.34° and 29.40°,which are characteristic peaks of $CaSO_4$ crystals. Spectrum (b) shows that the addition of the terpolymer has no influence on the crystal structure, which implies that only the surface morphology and particle size are changed in the presence of AA-APES-H_3PO_3.

3.9. The mechanism of scale inhibition

The results reported above indicate that the inhibitor functional groups exhibit a significant impact on the inhibitory power. In one molecule, the terpolymer AA-APES-H_3PO_3 contains –P(O)$(OH)_2$, –COOH, –SO_3 and PEG groups, among which both carboxylate and PEG segments are hydrophilic blocks and exist randomly in water [28]. On the one hand, the initial step is surface complexation

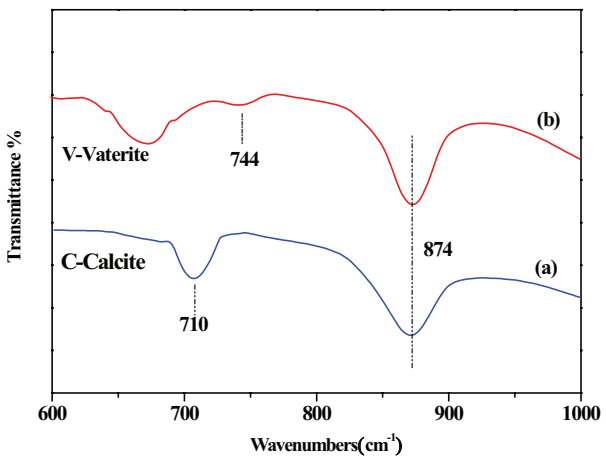

Fig. 10. FT-IR spectra of (a) $CaCO_3$ and (b) with the presence of 5 mg/L of AA-APES-H_3PO_3.

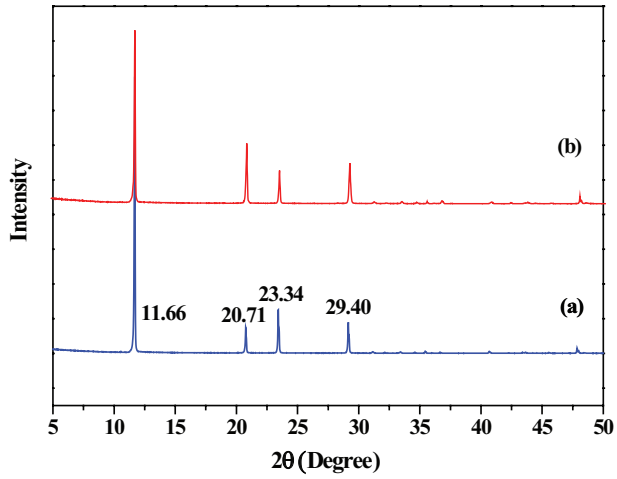

Fig. 12. XRD images for (a) $CaSO_4$ and (b) with the presence of 2 mg/L of AA-APES-H_3PO_3.

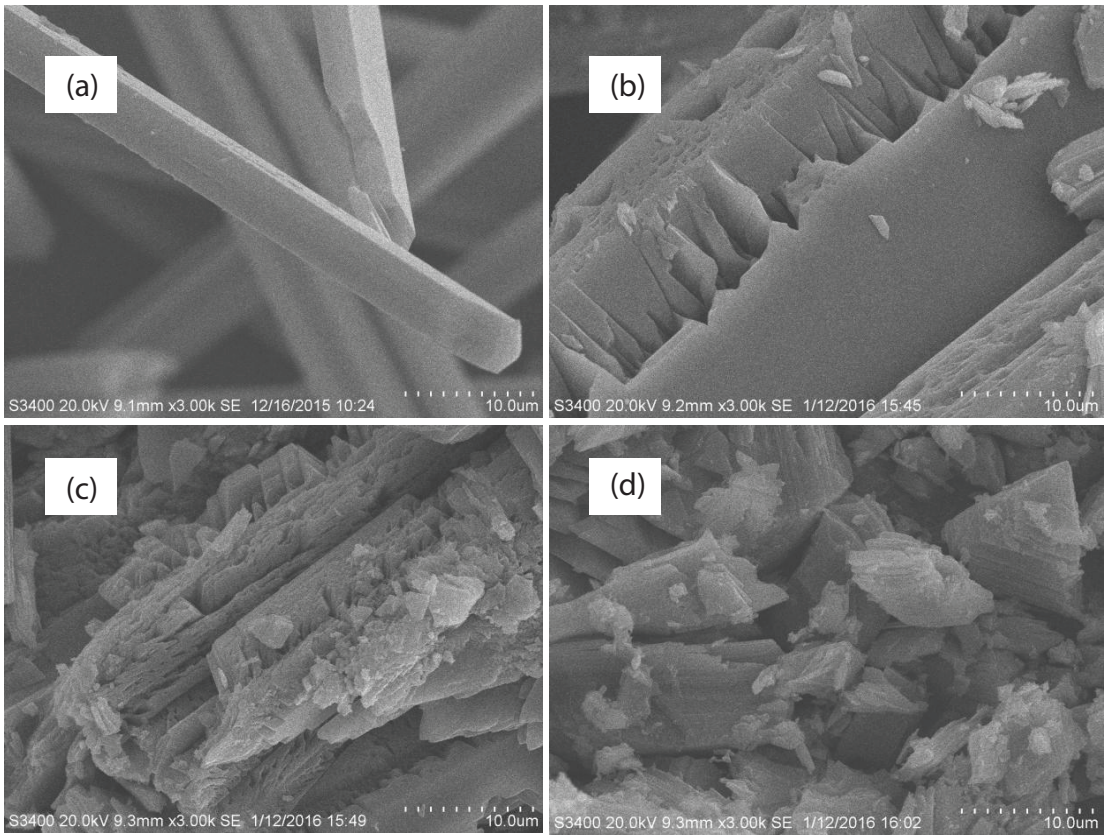

Fig. 11. SEM photographs for (a) $CaSO_4$ (b) with the presence of 1 mg/L, (c) 2 mg/L, (d) and 3 mg/L of AA-APES-H_3PO_3.

of the negatively charged polydentate ligand through its carboxylate or phosphonate moieties onto the positively charged Ca^{2+} lattice ions. In fact, the phosphonate group is doubly deprotonated so that the $–P(O)(OH)_2$ moiety bridges two Ca^{2+} centers. A part of the phosphonate group and the neighboring carboxylate group oxygen atoms at the PAA segments form a seven-membered chelate with the Ca^{2+} center, while the other part chelates Ca^{2+} with several carbonyl moieties in other molecule chains [13,29]. On the other hand, the terpolymer can strongly adsorb onto a $CaCO_3$ crystalline substrate owing to $–SO_3^-$ interaction with electric charge in the surface of crystal nucleus, disturbing the crystal growth due to the adsorption of the polymeric species at the active sites of crystal nucleus. Meanwhile, the $–SO_3^-$ groups can strengthen polymer solubility and then improve the extension of molecular chain, which encapsulate crystal nucleus more easily and steadily [15]. As a consequence, the structure of crystals can be significantly distorted and weakened.

4. Conclusions

A novel double-hydrophilic block terpolymer AA-APES-H_3PO_3 was prepared, and characterized by FT-IR and ^{1}H-NMR, which identifies that AA-APES-H_3PO_3 had the expected structure. The scale inhibition efficiency on $CaCO_3$ and $CaSO_4$ was investigated by static scale inhibition experiments. The results show that the AA-APES-H_3PO_3 terpolymer is effective in the calcium scales inhibition. The terpolymer exhibited 92.6% calcium carbonate inhibition at a threshold dosage of 8 mg/L, while it exhibited 97.9% calcium sulfate inhibition at a level of 4 mg/L. Moreover, the sharp falling in light transmittance from 100.0% to 19.4% was recorded and this revealed that AA-APES-H_3PO_3 was an effective dispersant. The morphology and crystal phase of $CaCO_3$ and $CaSO_4$ was characterized by SEM, XRD and FT-IR.

Acknowledgments

This work was supported by the National Natural Science Foundation of China (51673040), the Natural Science Foundation of Jiangsu Province (BK20171357), the Fundamental Research Funds for the Central Universities (2242018k30008,3207048418), Scientific Innovation Research Foundation of College Graduate in Jiangsu Province (KYLX16_0266, KYCX17_0134), a Project Funded by the Priority Academic Program Development of Jiangsu Higher Education Institutions (1107047002), Fund Project for Transformation of Scientific and Technological Achievements of Jiangsu Province of China (BA2016105), based on scientific research SRTP of Southeast University (T16192020), and the Scientific Research Foundation of Graduate School of Southeast University (YBJJ1417).

Reference

[1] Z. Amjad, P.G. Koutsoukos, Evaluation of maleic acid based polymers as scale inhibitors and dispersants for industrial water applications, Desalination, 335 (2014) 55–63.
[2] L.C. Wang, K. Cui, L.B. Wang, H.X. Li, S.F. Li, Q.L. Zhang, H.B. Liu, The effect of ethylene oxide groups in alkyl ethoxy carboxylates on its scale inhibition performance, Desalination, 379 (2016) 75–84.
[3] H.K. Can, G. Üner, Water-soluble anhydride containing alternating copolymers as scale inhibitors, Desalination, 355 (2015) 225–232.
[4] Z.F. Liu, S.S. Wang, L.H. Zhang, Z. Liu, Dynamic synergistic scale inhibition performance of IA/SAS/SHP copolymer with magnetic field and electrostatic field, Desalination, 362 (2015) 26–33.
[5] Y.M. Al-Roomi, K.F. Hussain, Application and evaluation of novel acrylic based $CaSO_4$ inhibitors for pipes, Desalination, 355 (2015) 33–44.
[6] J.H. Banga, Y.N. Janga, W. Kimb, K.S. Songa, C.W. Jeona, S.C. Chaea, S.W. Leea, S.J. Parkc, M.G. Leea, Precipitation of calcium carbonate by carbon dioxide microbubbles, Chem. Eng. J., 174 (2011) 413–420.
[7] L.F. Greenlee, F. Testa, D.F. Lawler, B.D. Freeman, P. Moulin, The effect of antiscalant addition on calcium carbonate precipitation for a simplified synthetic brackish water reverse osmosis concentrate, Water Res., 44 (2010) 2957–2969.
[8] Y.Y. Chen, Y.M. Zhou, Q.Z. Yao, Y.Y. Bu, H.C. Wang, W.D. Wu, W. Sun, Evaluation of a low-phosphorus terpolymer as calcium scales inhibitor in cooling water, Desal. Wat. Treat., 18 (2015) 945–955.
[9] J.X. Chen, L.H. Xu, H.N. Jian, S. Su, Q. Wu, Synthesis of modified polyaspartic acid and evaluation of its scale inhibition and dispersion capacity, Desalination, 358 (2015) 42–48.
[10] P. Kjellin, X-ray diffraction and scanning electron microscopy studies of calcium carbonate electrodeposited on a steel surface, Colloids Surf. A, 212 (2003) 19–26.
[11] X.R. Guo, F.X. Qiu, K. Dong, X. Zhou, J. Qi, Y. Zhou, D.Y. Yang, Preparation, characterization and scale performance of scale inhibitor copolymer modification with chitosan, J. Ind. Eng. Chem., 18 (2012) 2177–2183.
[12] F.S. De Souza, A. Spinelli, Caffeic acid as a green corrosion inhibitor for mild steel, Corros. Sci., 51 (2009) 642–649.
[13] Y.Y. Chen, Y.M. Zhou, Q.Z. Yao, Y.Y. Bu, H.C. Wang, W.D. Wu, W. Sun, Preparation of a low-phosphorous terpolymer as a scale, corrosion inhibitor, and dispersant for ferric oxide, J. Appl. Polym. Sci., 132 (2015). doi: 10.1002/APP.41447.
[14] M.S. Rahman, G.A. Gagnon, Bench-scale evaluation of drinking water treatment parameters on iron particles and water quality, Water Res., 48 (2014) 137–147.
[15] Y.Y. Bu, Y.M. Zhou, Q.Z. Yao, Y.Y. Chen, W. Sun, W.D. Wu, Preparation and evaluation of nonphosphate terpolymer as scale inhibitor and dispersant for $Ca_3(PO_4)_2$, $BaSO_4$, and Iron (III) hydroxide scales, J. Appl. Polym. Sci., 132 (2015). doi: 10.1002/APP.41546.
[16] S. Baklouti, M.R.B. Romdhane, S. Boufi, C. Pagnoux, T.Chartier, J.F. Baumard, Effect of copolymer dispersant structure on the properties of alumina suspensions, J. Eur. Ceram. Soc., 203 (2013) 905–911.
[17] K. Du, Y.M. Zhou, Y.Y. Wang, Fluorescent-tagged no phosphate and nitrogen free calcium phosphate scale inhibitor for cooling water systems, J. Appl. Polym. Sci., 113 (2009) 1966–1974.
[18] K. Du, Y.M. Zhou, L.Y. Da, Preparation and properties of polyether scale inhibitor containing fluorescent groups, Int. J. Polym. Mater., 57 (2008) 785–796.
[19] X.X. Gu, F.X. Qiu, X. Zhou, J. Qi, Y. Zhou, D.Y. Yang, Q. Guo, X.R. Guo, Synthesis and application of terpolymer scale inhibitor in the presence of β-cyclodextrins, J. Pet. Sci. Eng., 109 (2013) 177–186.
[20] C.E. Fu, Y.M. Zhou, J.Y. Huang, H.T. Xie, G.Q. Liu, W.D. Wu, Control of iron(III) scaling in industrial cooling water systems by the use of maleic anhydride–ammonium allylpolyethoxy sulphate dispersant, Adsorpt. Sci. Technol., 28 (2010) 437–448.
[21] S. Javad, A. Simin, Alkyl chain length, counter anion and temperature effects on the interfacial activity of imidazolium ionic liquids: comparison with structurally related surfactants, Fluid Phase Equilib., 386 (2015) 134–139.
[22] H. Elfil, H. Roques, Role of hydrate phases of calcium carbonate on the scaling phenomenon, Desalination, 137 (2001) 177–186.
[23] D. Liu, W.B. Dong, F.T. Li, Comparative performance of polyepoxysuccinic acid and polyaspartic acid on scaling inhibition by static and rapid controlled precipitation methods, Desalination, 304 (2012) 1–10.

[24] H.C. Wang, Y.M. Zhou, Q.Z. Yao, Y.Y. Bu, Y.Y. Chen, W. Sun, Study on calcium scales inhibition performance in the presence of double-hydrophilic copolymer, Inter. J. Polym. Mater., 64 (2015) 205–213.

[25] T. Chena, A. Nevillea, K. Sorbie, Z. Zhong, *In-situ* monitoring the inhibiting effect of polyphosphinocarboxylic acid on $CaCO_3$ scale formation by synchrotron X-ray diffraction, Chem. Eng. Sci., 64 (2009) 912–918.

[26] J.Y. Huang, G.Q. Liu, Y.M. Zhou, Q.Z. Yao, Y. Yang, Y. Ling, H.C. Wang, K. Cao, Y.H. Liu, P.X. Zhang, W.D. Wu, W. Sun, Acrylic acid–allylpolyethoxy carboxylate copolymer as an environmentally friendly calcium carbonate and iron(III) scale inhibitor, Clean Technol. Environ. Policy, 15 (2013) 677–685.

[27] P. Shakkthivel, R. Sathiyamoorthi, T. Vasudevan, Acrylic acid-diphenylamine sulphonic acid copolymer threshold inhibitor for sulphate and carbonate scales in cooling water systems, Desalination, 197 (2006) 179–189.

[28] C.E. Fu, Y.M. Zhou, G.Q. Liu, J.Y. Huang, W. Sun, W.D. Wu, Inhibition of $Ca_3(PO_4)_2$, $CaCO_3$, and $CaSO_4$ precipitation for industrial recycling water, Ind. Eng. Chem. Res., 50 (2011) 10393–10399.

[29] K.D. Demadis, P. Lykoudis, R.G. Raptis, G. Mezei, Phosphonopolycarboxylates as chemical additives for calcite scale dissolution and metallic corrosion inhibition based on a calcium-phosphonotricarboxylate organic–inorganic hybrid, Cryst. Growth. Des., 6 (2006) 1064–1067.